Topographic influences on development of Martian valley networks

Rossman P. Irwin III,[1,2] Robert A. Craddock,[3] Alan D. Howard,[4] and Holly L. Flemming[5]

Received 9 April 2010; revised 5 November 2010; accepted 23 November 2010; published 10 February 2011.

[1] Some morphometric differences between terrestrial and Martian valley networks may reflect the precursor topography on Mars, particularly impact basins or tectonic slopes. To evaluate these possible influences, we mapped highland watersheds in nine study areas that sample a range of geographic and topographic settings. We collected data including latitude, longitude, watershed length, divide and terminal elevations, watershed relief and slope, slope orientation, and qualitative descriptors including whether a drainage basin was open or closed. The longest valley networks and most overflowed basins occur on preexisting intercrater slopes of 0.1–1°, particularly on north facing slopes associated with the crustal dichotomy. The control of watershed length by earlier Noachian topographic features, which the relict networks did not significantly modify, suggests that the Early to Middle Noachian geomorphic environment was nominally much drier than the later Noachian to Hesperian transition. The distribution of fluvial valleys and likely orographic effects created by the crustal dichotomy suggest that evaporation from the northern lowlands was an important source of atmospheric humidity over short time scales. Much of the highland plateau consists of smaller enclosed watersheds, which (along with cooler temperatures) detained surface water at high elevations, lengthening or impeding the global water cycle. Ponding and evaporation may have partly offset a continentality effect of the highland landmass. Prolonged modification of the intercrater geomorphic surface prior to incision of valley networks included substantial weathering, reduction of relief, and gravity-driven sediment transport, indicating a long-term role for surface water in a transport-limited, arid to hyperarid Noachian paleoclimate.

Citation: Irwin, R. P., III, R. A. Craddock, A. D. Howard, and H. L. Flemming (2011), Topographic influences on development of Martian valley networks, *J. Geophys. Res.*, *116*, E02005, doi:10.1029/2010JE003620.

1. Introduction

[2] Martian valley networks and alluvial deposits are the most compelling evidence of a water cycle in the planet's early history, prior to ~3.7 Ga [e.g., *Fassett and Head*, 2008a]. Like their terrestrial analogs, Martian fluvial valleys follow topographic gradients and often originate near drainage divides, which lack contributing aquifers [e.g., *Carr*, 2002]. The broad spatial and topographic distribution of valley networks indicates an atmospheric water source [e.g., *Craddock and Howard*, 2002]. Prolonged impact crater degradation and landscape denudation suggest a significant water supply over geologic time [e.g., *Craddock et al.*, 1997; *Howard*, 2007] (Figure 1a). Aquifer recharge and/or overland flow were needed to erode the measured volumes of the valleys [*Howard*, 1988; *Gulick and Baker*, 1990; *Goldspiel and Squyres*, 1991; *Goldspiel et al.*, 1993; *Grant*, 2000]. Alluvial deposits on Mars occur at the mouths of some contributing valleys or densely dissected alcoves in crater rims [e.g., *Malin and Edgett*, 2003; *Moore and Howard*, 2005; *Irwin et al.*, 2005; *Hauber et al.*, 2009]. Large alluvial fans commonly have inverted paleochannels and morphometric properties that indicate deposition by normal fluvial erosion rather than debris flows [*Moore and Howard*, 2005].

[3] Over the last four decades, planetary literature has alternately emphasized the similarities and differences between terrestrial and Martian valley networks [e.g., *Masursky et al.*, 1977; *Pieri*, 1980; *Carr and Chuang*, 1997; *Mangold et al.*, 2004], but both sets of observations are valid and relevant to the paleoclimate. Martian valley networks typically have lower preserved drainage density, shorter lengths, relatively constant widths, low sinuosity, and poorly dissected to undissected intervalley surfaces [e.g., *Carr*, 1995; *Grant*, 2000; *Cabrol and Grin*, 2001] (review by *Irwin et al.* [2008]) (Figure 1). Their network structure reflects strong control by precursor topography (or locally by mapped structures),

[1]Planetary Science Institute, Tucson, Arizona, USA.
[2]Visiting scientist at Planetary Geodynamics Laboratory, NASA Goddard Space Flight Center, Greenbelt, Maryland, USA.
[3]Center for Earth and Planetary Studies, National Air and Space Museum, Smithsonian Institution, Washington, D. C., USA.
[4]Department of Environmental Sciences, University of Virginia, Charlottesville, Virginia, USA.
[5]MDA Information Systems Inc., Gaithersburg, Maryland, USA.

0148-0227/11/2010JE003620

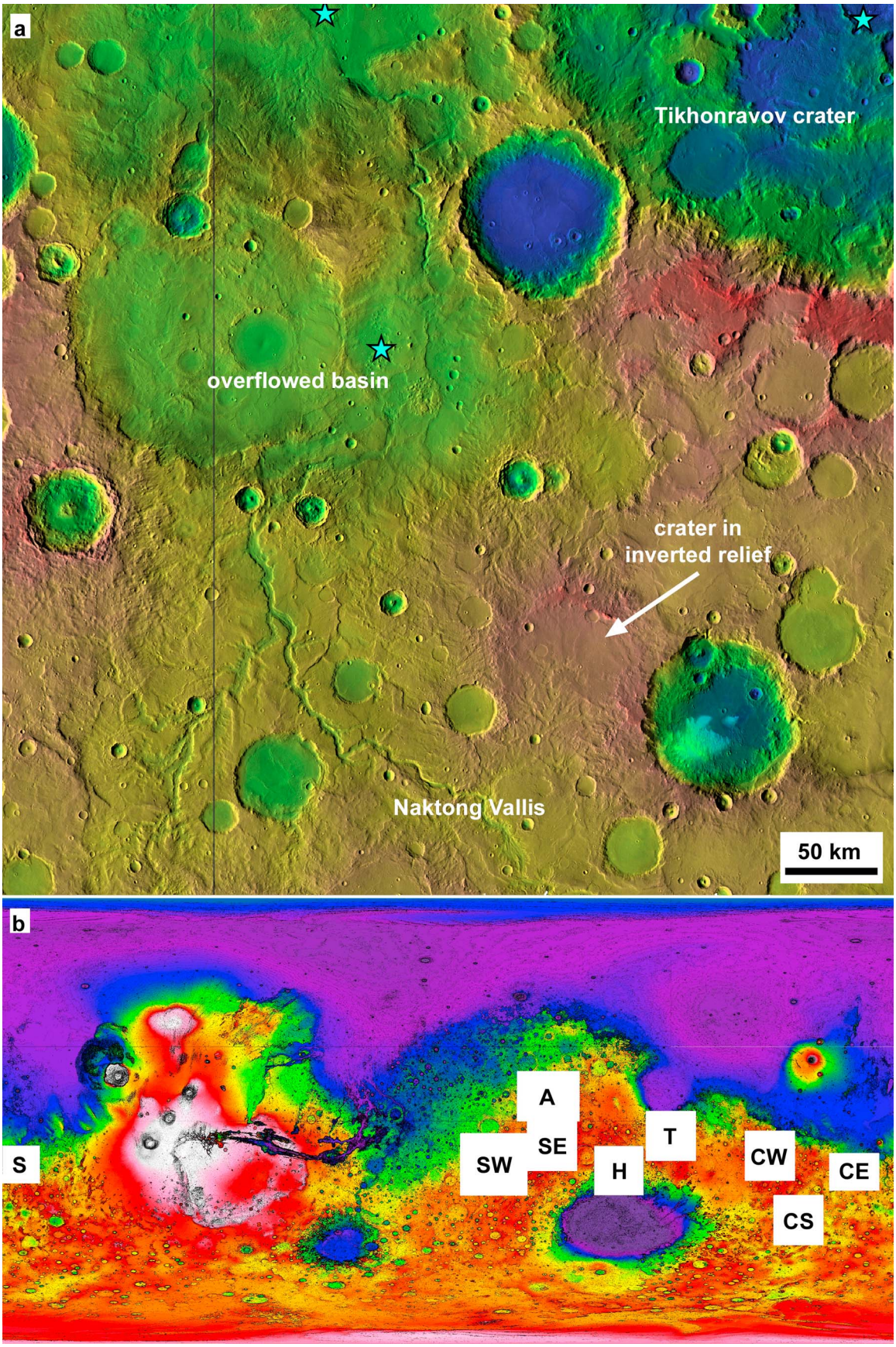
a
Tikhonravov crater
overflowed basin
crater in
inverted relief
Naktong Vallis
50 km
b
S
A
SW
SE
H
T
CW
CE
CS

Figure 1

and true dendritic patterns reflecting prolonged erosion of a homogeneous geological substrate are uncommon, particularly over larger spatial scales [*Pieri*, 1980]. Highly dissected landscapes with sharp divides between tributaries occur locally but are rare. Incision of depositional plains is not expected in most cases, but even most erosional slopes are not fully dissected. Valley topography is poorly graded relative to nominally concave longitudinal profiles on Earth [*Aharonson et al.*, 2002; *Kereszturi*, 2005; *Stepinski and Stepinski*, 2005; *Luo and Howard*, 2005]. The larger and denser valley networks on Mars often appear spatially clustered [*Carr*, 1995; *Gulick*, 2001].

[4] The immature development of Martian valley networks (by almost any measure) indicates that conditions favoring stream entrenchment were uncommon or geologically short lived [*Irwin et al.*, 2008]. Regardless of the prolonged erosion demonstrated by studies of Noachian impact craters [e.g., *Craddock and Maxwell*, 1993; *Grant and Schultz*, 1993; *Craddock et al.*, 1997; *Forsberg-Taylor et al.*, 2004], large alluvial deposits and their source valleys appear to have formed over shorter 10^4–10^6 year time scales [e.g., *Moore et al.*, 2003; *Moore and Howard*, 2005; *Bhattacharya et al.*, 2005; *Barnhart et al.*, 2009]. Development of large alluvial fans, breaching of formerly enclosed drainage basins, and entrenchment of rivers suggest that optimal conditions for fluvial activity prevailed around the Noachian-Hesperian transition [*Howard et al.*, 2005, *Irwin et al.*, 2005; *Fassett and Head*, 2008a] (throughout this paper, basin refers to a drainage basin unless it is specified as an impact basin). The implication is that prior and subsequent conditions were less favorable for valley incision, either due to less (or less intense) precipitation, higher infiltration capacity, higher rates of weathering and sediment production, or formation of a duricrust in the Late Noachian [*Howard et al.*, 2005].

[5] On Earth, the major controls on the amount of valley incision include bedrock resistance, precipitation, upslope contributing area, regional gradient, and smoothness of the initial topography. We must assume a similarly variable bedrock resistance between the two planets, given the limited relevant data from Mars. Contributing area is related to the length of the regional slope, gradient is easily measured, and precipitation is basically inferred by patterns unexplained by variations in the other three. It is more difficult to form integrated drainages through an irregular (e.g., cratered) surface.

[6] Entrenchment of a river requires excess sediment transport capacity (a function of stream power) relative to sediment supply, so it depends on discharge and slope, and inversely on the production and delivery of sediment from the surrounding slopes into the channel [e.g., *Simon and Darby*, 1999]. These requirements for stream entrenchment may yield some insight into why Martian valley networks appear spatially and temporally clustered. During earlier Noachian landscape degradation, streams apparently did not incise deeply or maintain sizable valleys over most of the landscape, suggesting a different balance of weathering and erosion. In the Late Noachian Epoch, larger and steeper slopes are hypothesized to have been more favorable for stream entrenchment during a geologically brief interval of wetter conditions.

[7] The purpose of this study is to evaluate the influence of precursor topography on the occurrence and length of Martian valley networks. If Pre-Noachian to Middle Noachian slopes and basins significantly influenced the development of Late Noachian to Early Hesperian valley networks, as we demonstrate below, then the climate must have been very arid with slow erosion rates throughout most of the Noachian Period, in order for ancient topography to persist long enough to control later valley development. Our results have broader implications for the source and transport of water vapor around the Noachian-Hesperian transition. Specifically, we examine the role of multibasin highland topography in lengthening or impeding the global water cycle, and the challenge in forming sizable valley networks on north facing regional slopes without a source of atmospheric humidity in the northern lowlands.

2. Methods

[8] We analyzed 54 watersheds in nine highland study areas (Figure 1b), which we selected to cover a wide range of geographic location, elevation, slope, and slope orientation (Table 1). We describe the study areas in section 3.

[9] For each study area, we prepared a 256 pixel/degree base mosaic including the Mars Odyssey Thermal Emission Imaging System (THEMIS) daytime infrared (DIR) mosaic 2.0, with missing data filled using the Viking Orbiter Mars Digital Image Mosaic (MDIM) 2.1. We colored the mosaics with Mars Orbiter Laser Altimeter (MOLA) topography to aid interpretation (e.g., Figure 2). Contour maps with 100 m intervals were based on the MOLA Mission Experiment Gridded Data Record (MEGDR) at 128 pixels/degree.

[10] We calculated idealized flow paths in these study areas using RiverTools 3.0 software and the 128 pixel/degree MEGDR. The resulting stream shapefiles assume fully integrated drainage, do not always trace real valley networks as seen in the imaging, and include the effects of post-Noachian landforms, so we did not use them for the measurements described below. Instead, we used the source areas of computationally derived headwater streams as a guide when

Figure 1. (a) Landforms in the Arabia study area (centered at 9°N, 34°E), including degraded Noachian impact craters, relatively smooth intercrater surfaces, incised valley networks, and fresh craters. Long, steep slopes commonly appear more densely dissected. One crater floor is elevated relative to its surroundings, and some larger basins to the northwest were heavily degraded prior to overflow by Naktong Vallis, suggesting that substantial denudation occurred in a more arid climate during the Noachian Period, until favorable conditions for valley entrenchment and basin overflow occurred near the Noachian-Hesperian transition [*Howard et al.*, 2005; *Irwin et al.*, 2005]. THEMIS daytime infrared mosaic 2.0 with missing data filled using the Viking Orbiter MDIM 2.1, with the topographic color scale as in Figure 2. (b) Global locator map in cylindrical projection of study areas (white boxes) shown relative to MOLA topography, centered on 0°N, 0°E. SW, Sabaea west; SE, Sabaea east; A, Arabia; H, Hellas; T, Tyrrhena; CW, Cimmeria west; CS, Cimmeria south; CE, Cimmeria east; S, Sirenum.

Table 1. Study Areas

Study Area	Longitude	Latitude	Description
Sabaea W	5–32°E	5–30°S	Plateau to NW slope, variably dissected, large grabens in SE
Sabaea E	32–52°E	0–20°S	Heavily dissected N slope, sparsely dissected plateau, large grabens in SE
Arabia	28–53°E	0–20°N	Long NW slope, most northern heavily dissected terrain
Hellas	59–79°E	10–30°S	Plateau to S slope into Hellas impact basin
Tyrrhena	80–100°E	4°N–16°S	Plateau to heavily dissected N slope into Isidis, steep mountain headwaters
Cimmeria W	120–140°E	4–24°S	Plateau to NE slope of crustal dichotomy
Cimmeria S	131.5–151.5°E	30–50°S	Most southern heavily dissected plateau
Cimmeria E	154–174°E	13–28°S	N slope of crustal dichotomy
Sirenum	180–195°E	10–25°S	Plateau and steep N slope of crustal dichotomy

manually mapping drainage divides (using ESRI ArcGIS 9.3 software at 1:2,000,000 scale), as long as the inferred divide was consistent with valleys observed in the imaging. We examined imaging of each subbasin within each watershed to determine whether it was part of an integrated network or drained internally. We focused on major drainage divides, so most mapped watersheds include smaller degraded craters and other basins that did not directly contribute surface water to the main valley network. Where our mapped divides end without closing a polygon, they indicate divides between major subbasins of a single watershed (e.g., flow converged near label 13 in Figure 2 in the upper reach of the Naktong Vallis watershed).

[11] To the extent possible, we mitigated the effects of post-Noachian fresh impact craters and faulting in interpretations of Noachian drainage pathways and divides. Interpreting past flow paths on Mars can be complicated, particularly on near-level surfaces where fresh impact craters have modified the topography or destroyed the old valley, or where substantial aeolian burial or deflation has occurred. Where large, fresh impact craters and their ejecta affected a significant area, the mapped drainage divide follows the shortest distance around the crater rim; the divide is likely inaccurate here but not overinterpreted, as the original divide is not preserved. Drainage divides are relatively precisely defined at sharp ridge crests, particularly along crater rims, but broad, low divides on intercrater plains are less precisely constrained. All drainage divides are thus approximate and interpreted with variable certainty across a given study area. These uncertainties may yield errors of up to a few percent in the length of a watershed along its stem valley. We did not measure dissected slopes that head at a fresh impact crater located on a precrater divide.

[12] The purpose of this analysis is to identify topographic controls on valley development, particularly factors that facilitated or limited the upper end of watershed length. For this reason, and in order to broaden our geographic scope, we collected data from only the largest watersheds in each study area, although many smaller watersheds and shorter valleys are also present. For each of 54 major watersheds, we assigned a number, took the latitude and longitude of the master stream at roughly the center of its watershed, and noted whether it was open (i.e., drained to the lowlands or Hellas) or closed. In some closed basins, ejecta from large fresh impact craters partly buried the longest flow path from the divide to the basin floor, so we measured the longest visible valley, which was typically no more than a few tens of kilometers shorter. We measured the watershed length as a straight-line distance from the divide to the mouth of the main valley (i.e., the point where the surface is no longer dissected), to avoid the effects of variable sinuosity, and we rounded the measurement to the nearest 10 km to avoid overstating the precision. In ArcGIS, we specified the planet and projection, so the length measurements are corrected for both factors. Where a watershed that began in a study area extended outside it, we measured the full length and relief of the watershed. We measured the relief from the divide to the valley mouth using the 128 pixel/degree MOLA MEGDR. Most drainage divides are highly irregular (subtending hundreds of meters) in elevation, and the recorded value is representative of the divide near the head of the master stream, but not the peak elevation. The valley-mouth elevation is better constrained to ±50 m, using measurements taken on plains immediately outside the valley mouth. The total relief (divide elevation minus valley mouth elevation) and the mean gradient of the watershed (relief divided by watershed length) were calculated from these data. The high and low elevations each incorporate some error, but the analysis below does not depend on precision, particularly in the irregular divide elevation. Finally, we tested the hypothesis that measurements from open and closed watersheds (length, divide elevation, relief, and gradient) were drawn from the same underlying probability distribution using a single-factor analysis of variance (anova) at the 95% confidence level. We note that these statistics pertain only to valley networks within our nine study areas, and a larger sample size may yield somewhat different results.

[13] We did not calculate watershed area, as most of the mapped watersheds contain Noachian craters or other depositional surfaces. Moreover, for closed drainage basins (which are the majority of those considered), the total watershed area is large relative to the length of any one radial interior stream, but very little of that area drained to the basin floor via the longest stream. The total area of closed drainage basins is thus not highly relevant to development of individual valleys.

3. Study Areas

[14] The following brief descriptions of each study area progress from west to east. Most of the areas are divided into well-integrated watersheds on long regional slopes and multibasin landscapes on the highland plateau. Likely open-basin paleolakes, where a basin has both a contributing network and an outlet valley [*Fassett and Head*, 2008b], are heavily concentrated on the regional slopes. In some cases, basin overflow around the Noachian-Hesperian transition integrated formerly enclosed watersheds in these areas.

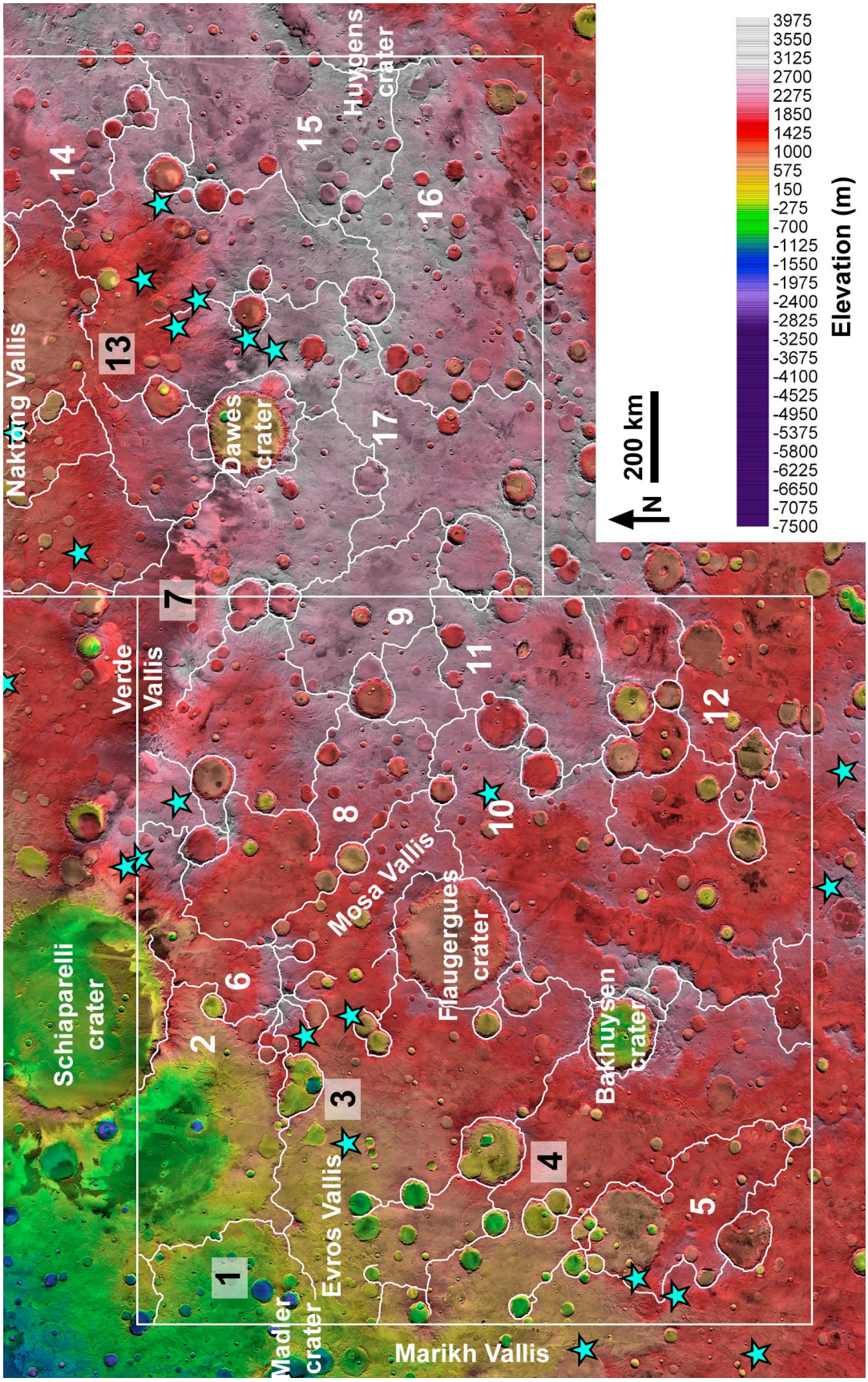

Figure 2. Numbered drainage basins and major features in the Sabaea west (5–32°E, 5–30°S) and Sabaea east (0–20°S, 32–52°E) study areas. White lines mark the study area boundaries and drainage divides, and blue stars note locations of breached basins (likely open-basin paleolakes) identified by *Fassett and Head* [2008b]. The topographic color scale applies to Figures 1–6, all of which are THEMIS daytime infrared mosaic 2.0 with missing data filled using the Viking Orbiter MDIM 2.1. Here and in Figures 3–6, closed watersheds are numbered with white text, and open ones are in black with a white background.

3.1. Sabaea West

[15] The Sabaea west study area (5–32°E, 5–30°S, Figure 2) is located on the southeastern side of the Chryse Trough. It includes a westward slope with well-integrated drainage mostly west of ~17°E (watersheds (W) W1, W3, and W4), and a multibasin highland landscape east of that meridian (W6, W8–W12). Most of the southwestern corner drained to the north via Marikh Vallis (W4) and the breached Mädler crater (125 km in diameter; hereafter length scales given after a crater name refer to its diameter), but some areas drained to large impact craters as terminal basins (W5, W6). The formerly west draining Mosa/Evros Vallis watershed (W3) covers much of the west central section. The topography of Schiaparelli crater (471 km) and a partially underlying impact basin (~530 km) (W2) dominates the northwestern corner. In the western part of the study area, drainage divides are primarily rims of large, degraded impact craters or low divides that are roughly parallel to the slope.

[16] The major divides between the westward slope and eastern plateau areas are related to a Hellas-circumferential graben in the south, Flaugergues crater (245 km) in the center, and Schiaparelli crater with its neighboring large basin in the north. The northeastern part of the area drained northward to the Verde Vallis watershed. Most of the divides separate early Noachian impact and intercrater basins, but large grabens circumferential to Hellas [*Solomon and Head*, 1980; *Wichman and Schultz*, 1989] also served as terminal basins. Bakhuysen crater (161 km) formed near the central drainage divide after most of the fluvial erosion had occurred. It and other large, internally draining craters are not included in the measurements.

3.2. Sabaea East

[17] About half of the Sabaea east study area (0–20°S, 32–52°E, Figure 2) drained to the north via Naktong and Verde Valles (W13) to its west. The southern and eastern parts of the area (W14–W17) are multibasinal, dominated by ancient impact and intercrater basins as well as large Hellas-circumferential grabens. The circum-Hellas divide, separating watersheds that drained toward the northern lowlands from those that drained toward Hellas, also separates distinct styles of erosion. Drainage toward the lowlands (W13) is denser and better integrated, whereas the Hellas-oriented networks to the southeast (W16, W17) are commonly short, endorheic, and sparse. The rim of Huygens crater (470 km) is a major divide on the southeastern boundary of the area, but low intercrater rises form most of the hydrologic divides. The youngest large crater in this area is Dawes (191 km), but it has a buried central peak and heavily dissected walls, attesting to its Noachian age. Dawes crater forms part of the divide between the Naktong (W13) and Verde Vallis (W7) watersheds.

3.3. Arabia

[18] Of the nine study areas, Arabia (0–20°N, 28–53°E, Figure 3) has the largest fraction of its area within a single drainage basin (W13). Aside from the southeastern corner (W14) and some impact craters, nearly the entire area drained to the lowlands via the Naktong/Scamander/Mamers valley network and its tributary, Indus Vallis. The northeastern quarter of the area that lies within the Indus Vallis watershed has undergone significant (likely aeolian) burial and partial exhumation [*Greeley and Guest*, 1987; *Grant and Schultz*, 1990; *Moore*, 1990; *Fassett and Head*, 2007], complicating the mapping of drainage divides (specifically, whether Locras and Cusus Valles in the northeast fed Indus Vallis, as appears likely). These large drainage basins were not completely integrated throughout most of the Noachian Period. Divides between multiple enclosed basins were breached around the Noachian-Hesperian transition (Figure 1), presumably due to a greater influx of water from the region around Dawes crater to the south [*Irwin et al.*, 2005].

[19] Drainage divides in the Arabia study area include a combination of ancient impact-basin rims, visible crater rims, intercrater divides, and the partially buried and exhumed Tikhonravov crater (386 km). Enclosed drainage is restricted primarily to Noachian impact craters and the plateau in the southeastern corner of the study area.

3.4. Hellas

[20] A north-south distinction in valley network planform is evident between the Arabia and Hellas study areas. On the intercrater surfaces in Arabia, the long slopes are more densely dissected, but stem valleys also deeply incise some low-gradient plains. In contrast, the Hellas study area (10–30°S, 59–79°E, Figure 4) retains large, enclosed drainage basins and undissected plains over half of its area (W18–W22), despite a significant regional gradient of ~0.005 (0.3°) on cratered terrain above −3 km in elevation. Fluvial dissection is concentrated at higher elevations, particularly north of 20°S. The poorly integrated drainage from north to south could be attributable to lower long-term runoff production rates or to the unusually large area of enclosed basin floors in this study area. Most of the valley networks in the north debouch to these large plains, which would require high runoff production rates to exceed evaporation and overflow.

[21] Some authors have discussed a possible inland sea in Hellas, the deepest basin on Mars, with a range of possible levels between +600 and −6000 m [e.g., *Moore and Wilhelms*, 2001; *Wilson et al.*, 2007, 2010]. It is difficult to envision a situation where water eroded valleys in the highlands but did not collect in Hellas. However, constraining the water depth in Martian basins without obvious outlet valleys is notoriously challenging, particularly before the Noachian-Hesperian transition. Several Late Noachian to Hesperian impact craters around 22°S have large alluvial fans with toes as low as −2800 m in elevation [*Moore and Howard*, 2005], suggesting that relatively intense precipitation was available at lower elevations and higher latitudes in Hellas around that time, although this development would not necessarily require frequent rain. There is remarkably little fluvial dissection of a steeper (0.05 or 3°) slope into Hellas below about −3 km. Normally, rivers flowing from a gentle surface to a steeper one become more erosive, which should create a more heavily dissected surface that is not observed at low elevations within the basin [*Wilson et al.*, 2010]. However, the sparse occurrence of valley networks south of ~20°S may be partly attributable to post-Noachian terrain softening or mantling.

[22] Drainage divides in this study area are more often related to Hellas mountain belts and structures than to

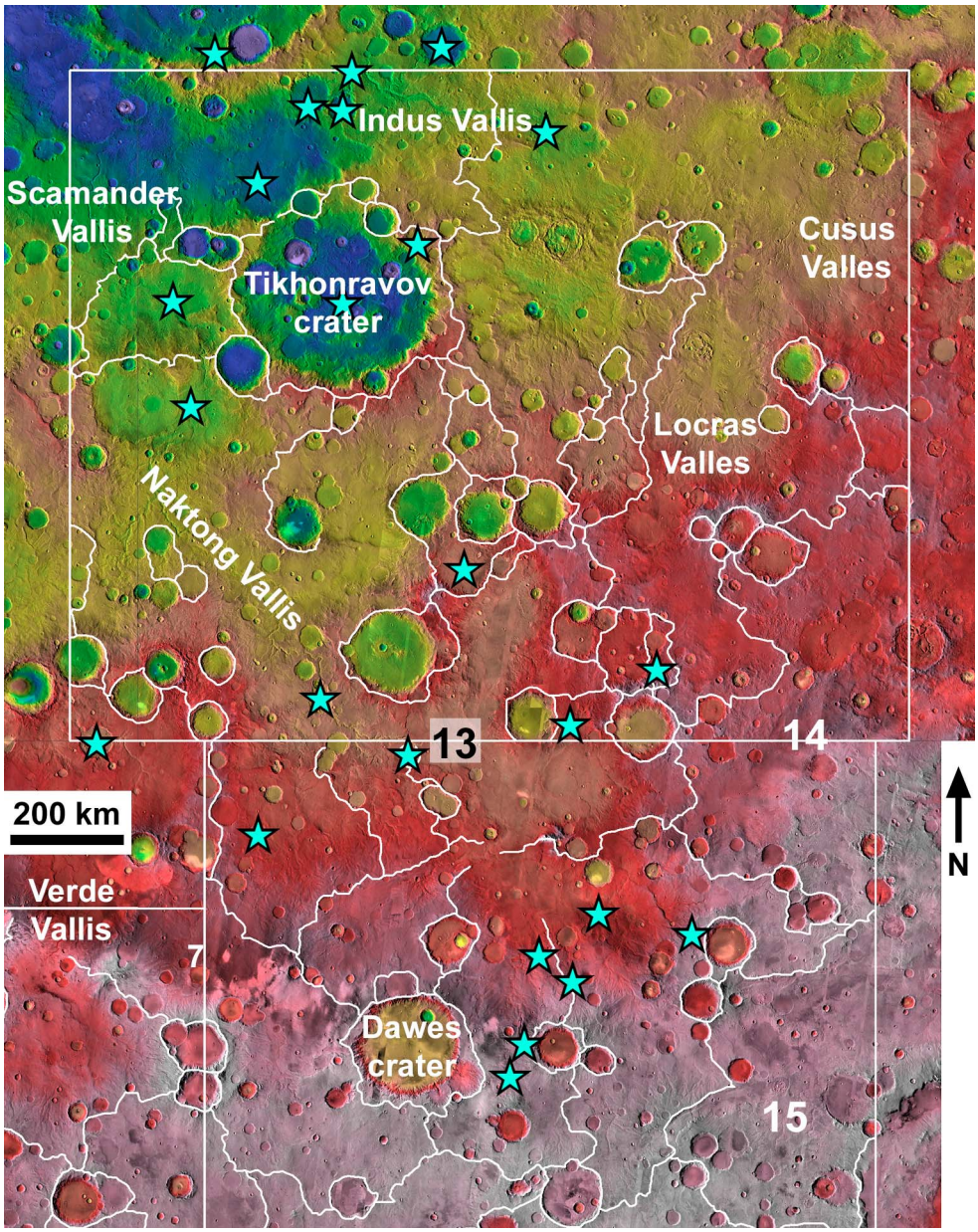

Figure 3. Numbered drainage basins and major features in the (top) Arabia (0–20°N, 28–53°E) and (bottom) northern Sabaea east study areas.

impact craters, but Huygens crater and an older, highly degraded impact basin to the east (W18) are important topographic divides in the northwestern corner.

3.5. Tyrrhena

[23] Northeast of Hellas, the densely dissected Tyrrhena area (16°S–4°N, 80–100°E, Figure 4) includes a northward slope through Libya Montes to Isidis impact basin (W24), but the Tyrrhena Terra plateau (southwestern and south central part of the study area) is less dissected and largely endorheic (W26, W27). The southeastern watershed (W28) drained off the plateau toward Hesperia Planum. Nearly all of the breached impact craters that contain both contributing and outlet valleys as noted by *Fassett and Head* [2008b] are in the northern watershed (W24) that drained to Isidis. This study area has more fluvial dissection, more breached craters, longer drainage basins, and better integration of the landscape than does the Hellas study area, which is similarly situated on the margin of a large impact basin. Structures and mountain belts related to Isidis basin are more significant sources of drainage divides than are visible impact craters, none of which exceeds 100 km in diameter in this area. *Howard et al.* [2005] mapped valley networks in this area, noting a similar pattern.

3.6. Cimmeria West

[24] The Cimmeria west, Cimmeria east, and Sirenum study areas include parts of the cratered slope between the highland plateau and the northern lowlands. The slope in the cratered terrain is relatively steep, resulting in shorter valley

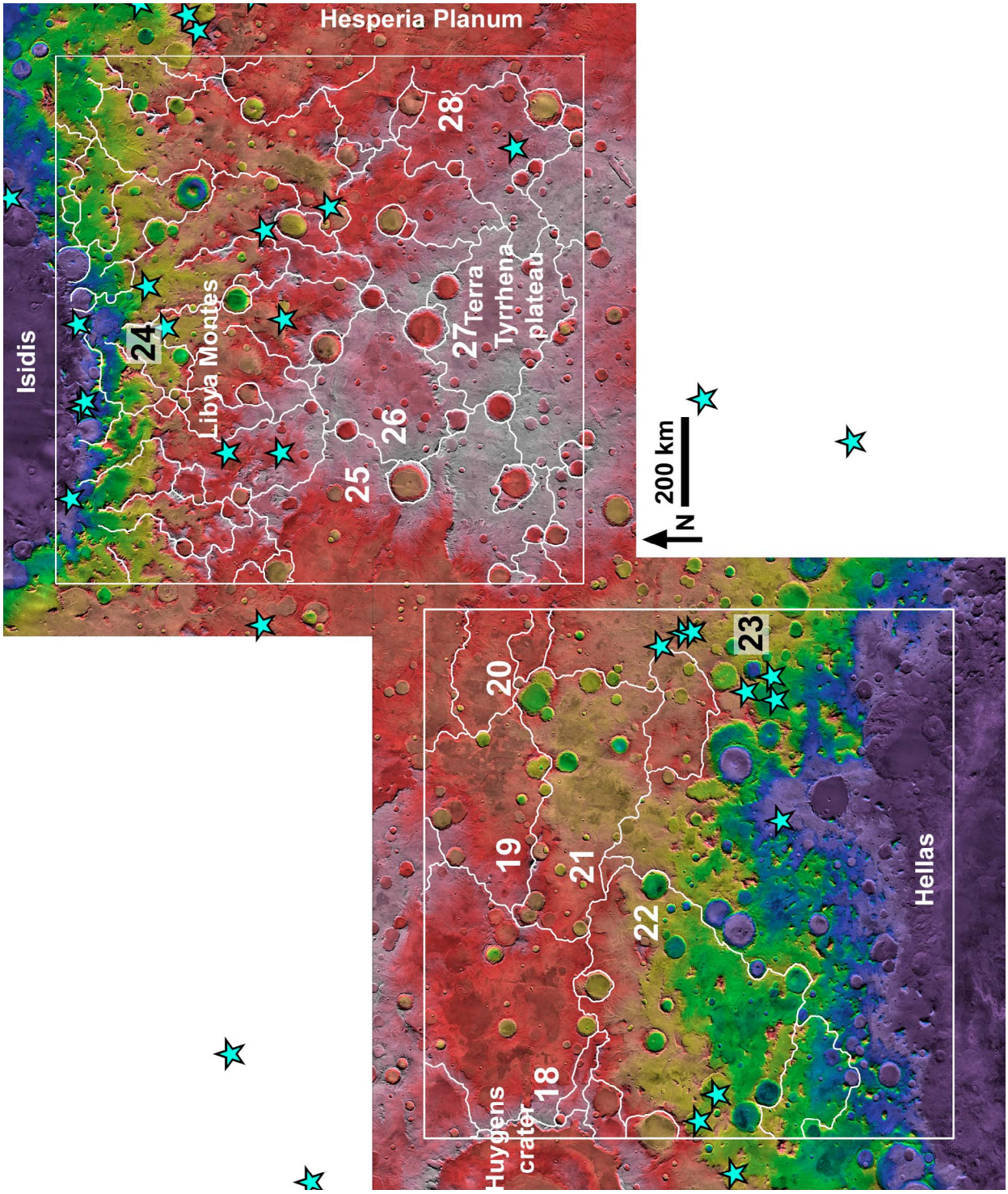

Figure 4. Numbered drainage basins and major features in the Tyrrhena (16°S–4°N, 80–100°E) and Hellas (10–30°S, 59–79°E) study areas.

networks per unit of relief and more endorheic surface area on the plateau, relative to study areas on the more gradual slope from the highland plateau into the Chryse Trough and Arabia Terra. The Cimmeria west area (4–24°S, 120–150°E, Figure 5a) includes some watersheds (including Licus Vallis, W29) that drained across the crustal dichotomy boundary scarp into the lowlands, as well as one watershed (W31) that debouched to Gale crater (155 km). Most of the drainage basins to the south (W30, W32–W35) are enclosed, and the divides are related to early Noachian impact basins or older topographic ridges of unknown origin as well as many smaller impact craters. The dominant central feature is the Herschel impact basin (305 km). *Irwin and Howard* [2002] described the interaction between impact cratering and fluvial erosion in shaping this landscape during the Noachian Period, noting that the underlying topography had a significant effect on crater degradation and sediment transport pathways.

3.7. Cimmeria South

[25] The Cimmeria south study area (30–50°S, 131.5–151.5°E, Figure 5b) is located on the highland plateau east of Hellas basin. It contains relatively dense valley networks, which are otherwise uncommon at high southern latitudes. The topographic divides and endorheic drainage are almost entirely related to early Noachian impact basins or smaller superimposed craters (W36–W44), but old Hellas-concentric grabens control flow patterns in the southeastern corner. An important feature in the southern part of the study area is the Kepler impact basin (233 km).

3.8. Cimmeria East

[26] The Cimmeria east area (13–28°S, 154–174°E, Figure 6a) is similar to Cimmeria west in many respects, but it contains two large stem valleys (Al-Qahira and Durius Valles, W45 and W48, respectively) that greatly exceed the size of most other Noachian fluvial valleys on Mars. Early classification schemes for valley networks recognized a distinction between the common "small" valleys (widths of ~0.5–5 km and depths of ~50–350 m) and several larger stem valleys (~10 km wide and >500 m deep, e.g., Ma'adim, Durius, Al-Qahira, Licus, and several on the northern side of Arabia Terra) [*Masursky*, 1973; *Sharp and Malin*, 1975; *Masursky et al.*, 1977]. These valleys represent larger or more prolonged discharges of water, possibly due to a topographic configuration that facilitated downcutting and/or collection of water from a large area (see section 5.1).

[27] The most important topographic feature in the Cimmeria east study area is a divide that trends SSW-NNE and includes a number of ~50–100 km impact craters. Watersheds W46 and W47 to the south drain internally. The major drainage divides to the north are low intercrater divides and rims of impact craters.

3.9. Sirenum

[28] The Sirenum study area (10–25°S, 180–195°E, Figure 6b) includes one of the steepest cratered slopes along the crustal dichotomy boundary, which dominates the drainage pattern in the northwestern side of the study area (W49, W50). The divide mentioned in the Cimmeria east area continues into the northwestern corner of the Sirenum area. The eastern border of the area is a broad trough (W54) that drained from south to north and was fed by tributaries from the major watersheds in the east central section. This low-lying surface may be tectonic in origin or could be a relict relief feature from large, very highly degraded impact basins that formed during the early Noachian. The southern and southwestern parts of the area are a multibasinal plateau (W51–W53), contiguous with a broad, elongated rise that is oriented SE-NW and subtends about 60° of an arc circumferential to Tharsis. It is not certain whether there is a causal relationship, but the rise could be related to Tharsis loading [*Phillips et al.*, 2001].

4. Results

4.1. Watershed Length

[29] Table 2 includes data from 54 drainage basins within the nine study areas. For closed watersheds, the length is the distance from the divide near the head of the master stream to the margin of the terminal basin, rounded to the nearest 10 km. These lengths (Figure 7) vary from 40 to 370 km in the study areas, plus a watershed (W31) that is 550 km long and may have been open to the lowlands before Gale crater formed and became its terminal basin. Open basins can be larger, with lengths of 310 km to over 1,000 km in four cases (three of which are included in Figure 7; the fourth (W13) is 3350 km long), exceeding the dimensions of the study areas. The single-factor anova rejected the hypothesis at the 95% level that that length measurements from open and closed basins were drawn from the same underlying probability distribution (p value = $1*10^{-7}$). There are shorter open watersheds on Mars as well, down to ~100 km length scales, particularly along steep margins of the Isidis basin and the crustal dichotomy boundary in Terra Sirenum. The closed highland basins limit the length of the valleys within them to <300–400 km. These measurements are consistent with prior studies, which reported valley lengths of tens to hundreds of kilometers [*Carr and Clow*, 1981; *Baker and Partridge*, 1986; *Carr*, 1995; *Cabrol and Grin*, 2001].

[30] Some open watersheds are longer in part due to overflow and breaching of enclosed basins downstream (e.g., W4, W13, W24, W31, W50, and W54). The overflowed impact craters and other basins reported by *Fassett and Head* [2008b] are heavily concentrated on the northward slope of the crustal dichotomy (Figures 2–6), where the landscape was more favorable for concentrating enough runoff to fill and overflow the basins. The plateau to the south, where slopes are shorter, has relatively few breached basins with outlet valleys, and those breached basins tend to be small craters < 40 km in diameter.

4.2. Elevation, Relief, Slope, and Slope Orientation

[31] The divide elevations, which are highly variable within each watershed and imprecisely measured here, appear broadly similar for open and closed watersheds, but the terminal elevations of open watersheds are commonly lower (Figure 8). The single-factor anova failed to reject the hypothesis at the 95% level that that divide elevations from open and closed basins were drawn from the same underlying probability distribution (p value = 0.159). Of the 41 closed watersheds, 37 have terminal elevations (where the master stream is no longer entrenched) ranging from 450 to 2600 m, whereas 12 of 13 open networks end at −250 to −3700 m. For

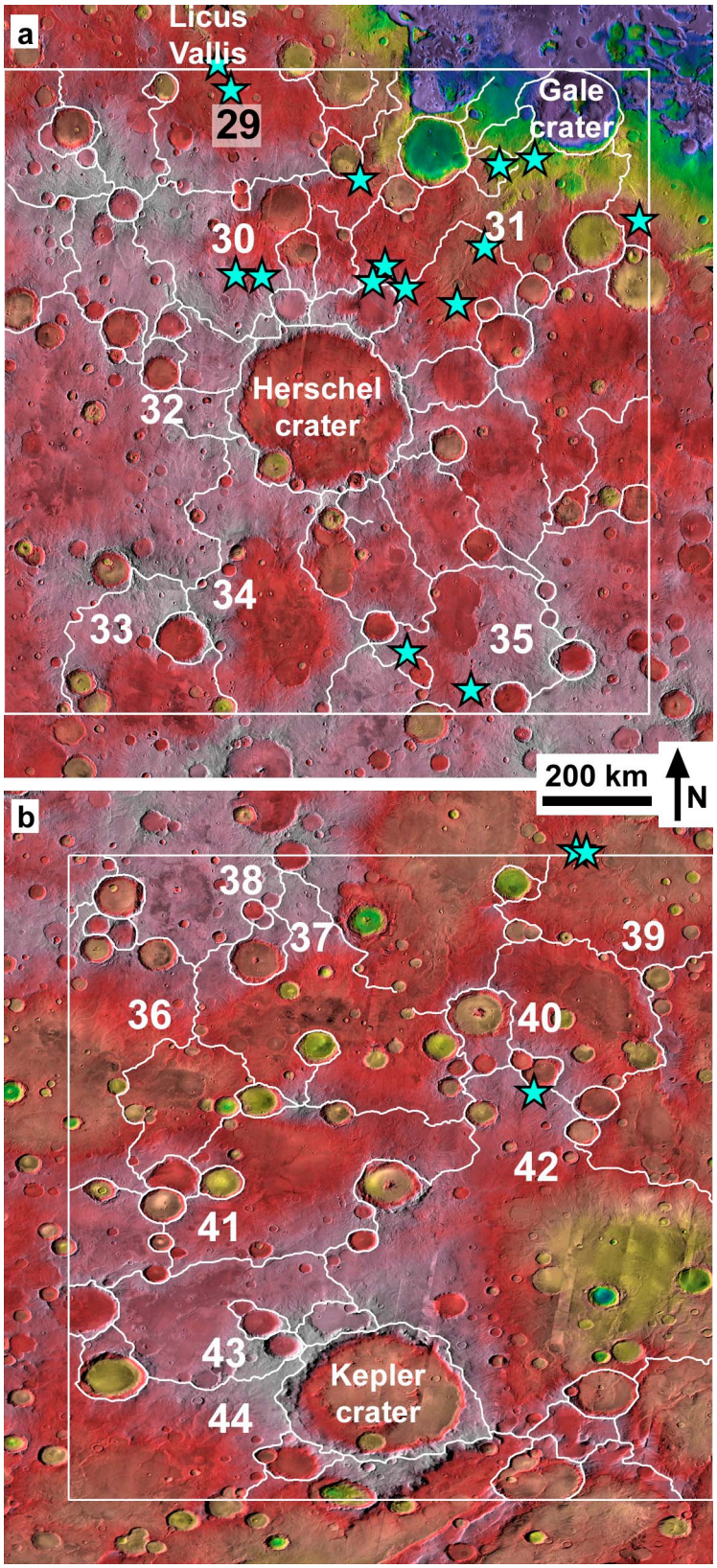

Figure 5. Numbered drainage basins and major features in the (a) Cimmeria west (4–24°S, 120–150°E) and (b) Cimmeria south (30–50°S, 131.5–151.5°E) study areas.

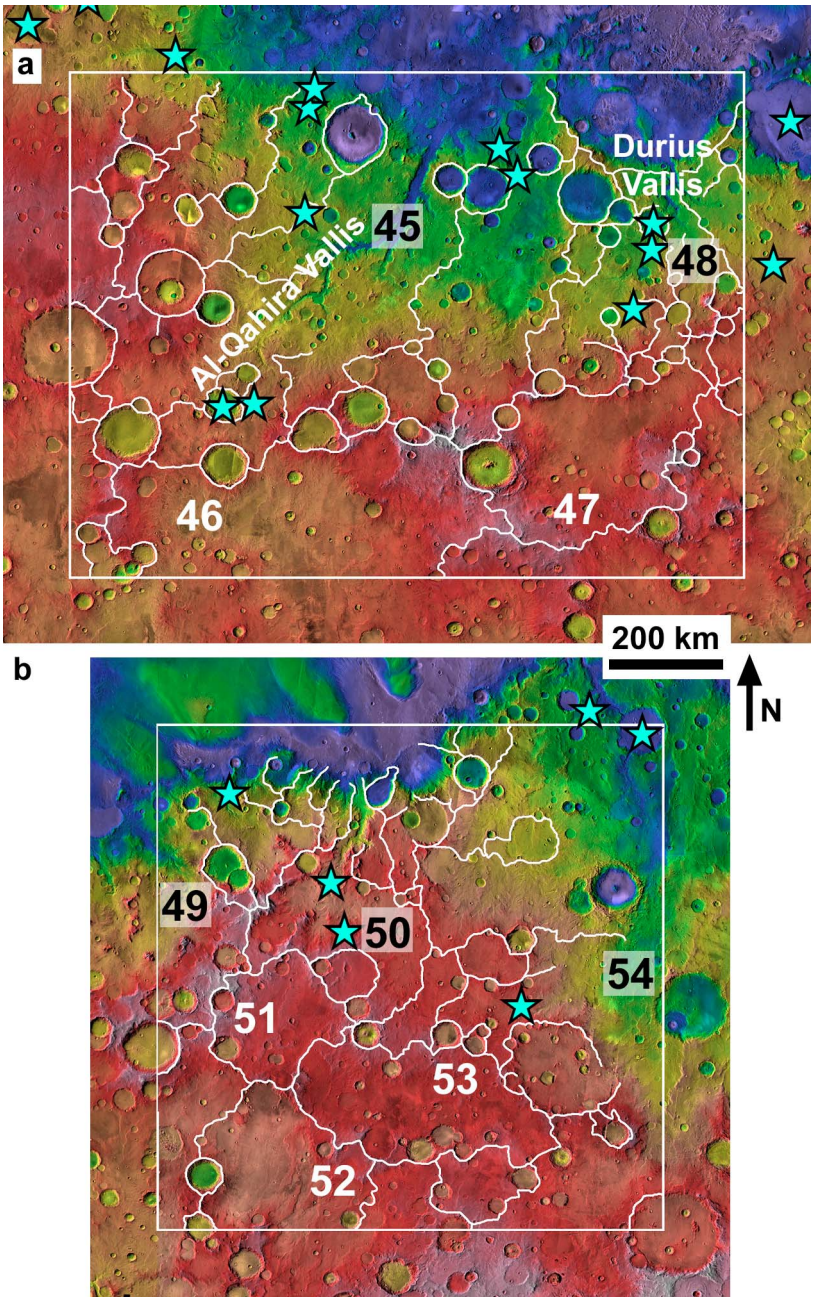

Figure 6. Numbered drainage basins and major features in the (a) Cimmeria east (13–28°S, 154–174°E) and (b) Sirenum (10–25°S, 180–195°E) study areas.

Table 2. Morphometric Data for 54 Selected Watersheds[a]

Study Area	W#	Open or Closed	Latitude (°N)	Longitude (°E)	Length (km)	Source	Elevation High (m)	Elevation Low (m)	Relief (m)	Slope	Flow to	Notes
Sabaea W	1	open	−8.9	7.0	710	CD	550	−1460	2010	0.0028	W	In area: L = 220 km, low = −750 m.
Sabaea W	2	closed	−7.5	15.5	220	HB,CD	1500	−500	2000	0.0091	W/N	Max. length to floor of 530 km Early Noachian basin. Divide ~1200 to 1800 m.
Sabaea W	3	open	−12.6	14.0	1100	CD	2100	−150	2250	0.0020	W	Mosa/Evros Valles, includes overflowed basin between them. Length in study area. Appears to continue beyond fresh craters.
Sabaea W	4	open	−19.5	10.0	1800	CD	2250	−1460	3710	0.0021	N	Marikh Vallis, through Mädler crater. In area: L = 1250, low = −1150.
Sabaea W	5	closed	−25.7	9.4	320	CD,C	1700	700	1000	0.0031	NW	Drained to unnamed crater D~178 km.
Sabaea W	6	closed	−7.0	18.7	320	CD,IB	2500	−200	2700	0.0084	N	Brazos Vallis, drained to Schiaparelli crater.
Sabaea W	7	open?	−9.0	34.3	920	CD	2800	700	2100	0.0023	NW	Verde Vallis. Length to breached crater where low elevation taken. Possible lower reach destroyed by crater at 1.5N, 27E.
Sabaea W	8	closed	−12.0	22.5	370	CD	2500	1300	1200	0.0032	NW	May have connected to watershed W6, in which case L~730 km and low elevation is −200 m.
Sabaea W	9	closed	−15.0	31.0	80	HB	2750	2450	300	0.0038	N	Enclosed highland basin.
Sabaea W	10	closed	−18.0	24.5	280	G	2450	1450	1000	0.0036	SW	Drained to a large graben.
Sabaea W	11	closed	−21.3	26.4	190	HB	2650	1850	800	0.0042	E	Enclosed highland basin.
Sabaea W	12	closed	−25.6	28.0	120	HB,C	2250	950	1300	0.0108	E	Enclosed highland basin.
Sabaea E	13	open	0.0	38.1	3350	CD	2900	−3700	6600	0.0020	N	Headwater S of Dawes to end of Mamers Vallis. In area: L = 1550, low = −350.
Sabaea E	14	closed	0.0	50.0	220	HB,C	2500	1350	1150	0.0052	N	Enclosed highland basins.
Sabaea E	15	closed	−11.0	49.5	190	HB	2800	2300	500	0.0026	NE	Enclosed highland basins.
Sabaea E	16	closed	−16.0	46.3	230	G	3100	2100	1000	0.0043	S	Drains to grabens NW of Hellas.
Sabaea E	17	closed	−14.2	37.5	50	HB	2900	2600	300	0.0060	S	Enclosed basin with very little relief on the margins.
Hellas	18	closed	−11.0	67.0	140	HB	2200	1500	700	0.0050	W	Enclosed basin near east rim of Huygens crater.
Hellas	19	closed	−13.4	69.0	180	HB	1900	950	950	0.0053	E	Enclosed basin outside rim of Hellas basin.
Hellas	20	closed	−13.2	76.8	40	HB	1500	1000	500	0.0125	N	Enclosed basin outside rim of Hellas basin.
Hellas	21	closed	−15.7	69.0	240	H	1500	450	1050	0.0044	E	Enclosed basin outside rim of Hellas basin.
Hellas	22	closed	−18.0	67.0	240	H	1500	−750	2250	0.0094	S	Dissection on north rim of Hellas basin.
Hellas	23	open	−18.0	78.3	640	H	1600	−1450	3050	0.0048	S	Large drainage basin NE of Hellas, drained to area near Terby crater.
Tyrrhena	24	open	1.0	90.9	700	I	2700	−3600	6300	0.0090	N	Numerous valley networks draining directly to Isidis basin.
Tyrrhena	25	closed	−7.1	83.0	220	U	2700	1200	1500	0.0068	W	Drains west off Tyrrhena plateau.
Tyrrhena	26	closed	−8.6	86.0	190	HB	3200	2100	1100	0.0058	E	Enclosed basin on Tyrrhena plateau.
Tyrrhena	27	closed	−12.2	88.2	100	HB	3200	2100	1100	0.0110	N	Enclosed basin on Tyrrhena plateau.
Tyrrhena	28	closed?	−10.5	98.0	380	U	2800	1200	1600	0.0042	E	Drains east off Tyrrhena plateau.
Cimmeria W	29	open	−6.0	126.7	470	CD	2500	−500	3000	0.0064	N	Extends outside of map area to end of Licus Vallis.
Cimmeria W	30	closed	−10.0	127.8	220	CD	2800	1100	1700	0.0077	NE	Drains to a 92 km crater, which may have overflowed. A fresh crater overlies the outlet.
Cimmeria W	31	closed	−10.0	134.2	550	CD	2300	−4500	6800	0.0124	NE	Between rim of Herschel crater and floor of Gale crater.
Cimmeria W	32	closed	−14.5	124.7	150	HB	2500	2000	500	0.0033	W	Closed basin west of Herschel crater.
Cimmeria W	33	closed	−21.5	123.1	100	HB	2300	1700	600	0.0060	SE	Enclosed highland basin.
Cimmeria W	34	closed	−20.4	127.0	110	HB	3000	1400	1600	0.0145	E	Heavily dissected enclosed basin SW of Herschel crater.
Cimmeria W	35	closed	−21.4	135.8	150	HB,C	2800	1650	1150	0.0077	W	Enclosed highland basin, drains to crater.
Cimmeria S	36	closed?	−34.7	134.0	210	HB	2200	1000	1200	0.0057	SW	Drained to plains contiguous with southern Hesperia Planum. May have formerly drained toward Hellas.
Cimmeria S	37	closed	−32.6	139.0	160	HB	2900	1450	1450	0.0091	S	Possible overflow of one large basin to another due to infilling. Fresh crater crosscuts lower reach, original length possibly 220 km.
Cimmeria S	38	closed	−31.0	137.2	110	HB	2800	2200	600	0.0055	W	Enclosed highland basin.
Cimmeria S	39	closed	−31.5	148.6	150	HB	1600	900	700	0.0047	N	Enclosed highland basin.
Cimmeria S	40	closed	−35.0	146.0	100	HB	2200	1350	850	0.0085	N	Enclosed highland basin.

Table 2. (continued)

Study Area	W#	Open or Closed	Latitude (°N)	Longitude (°E)	Length (km)	Source	Elevation High (m)	Elevation Low (m)	Relief (m)	Slope	Flow to	Notes
Cimmeria S	41	closed	−41.7	136.0	110	HB	2300	1600	700	0.0064	NE	Enclosed highland basin.
Cimmeria S	42	closed	−38.3	145.5	320	HB	2300	550	1750	0.0055	S	Enclosed highland basin.
Cimmeria S	43	closed	−45.3	136.3	110	HB	3300	2050	1250	0.0114	W	Enclosed highland basin.
Cimmeria S	44	closed	−47.0	136.8	210	HB	3500	1450	2050	0.0098	SW	Enclosed highland basin.
Cimmeria E	45	open	−18.0	163.3	750	CD	1500	−1550	3050	0.0041	NE	Al-Qahira Vallis.
Cimmeria E	46	closed	−26.0	157.0	190	HB	1900	650	1250	0.0066	E	Enclosed highland basin.
Cimmeria E	47	closed	−26.5	169.1	170	HB	2000	1100	900	0.0053	NE	Enclosed highland basin, longest valleys mostly buried by ejecta.
Cimmeria E	48	open	−18.0	172.5	310	CD,IB	2200	−1600	3800	0.0123	N	Central branch Durius Vallis. Highly irregular drainage divide.
Sirenum	49	open	−14.1	−179.5	340	CD	2200	−1400	3600	0.0106	N	Crosses dichotomy boundary.
Sirenum	50	open	−14.0	−174.5	430	CD,HB	1900	−2000	3900	0.0091	N	Crosses dichotomy boundary.
Sirenum	51	closed	−19.0	−177.9	50	HB	2400	1700	700	0.0140	E	Enclosed highland basin.
Sirenum	52	closed	−24.3	−174.5	140	HB	1900	1000	900	0.0064	SW	Enclosed highland basin.
Sirenum	53	closed	−20.0	−171.4	60	HB	1800	1450	350	0.0058	S	Enclosed highland basin, includes small subbasins.
Sirenum	54	open	−18.7	−165.4	1300	U, CD	2800	−2000	4800	0.0037	N	Basin extends outside study area to N and S.

[a]W# is watershed number. Source of slope: CD, crustal dichotomy; HB, highland basin (highly degraded); IB, impact basin, less degraded with steep inner walls; C, small degraded crater; G, graben; H, Hellas; I, Isidis; U, slope off regional-scale topographic feature of unknown origin.

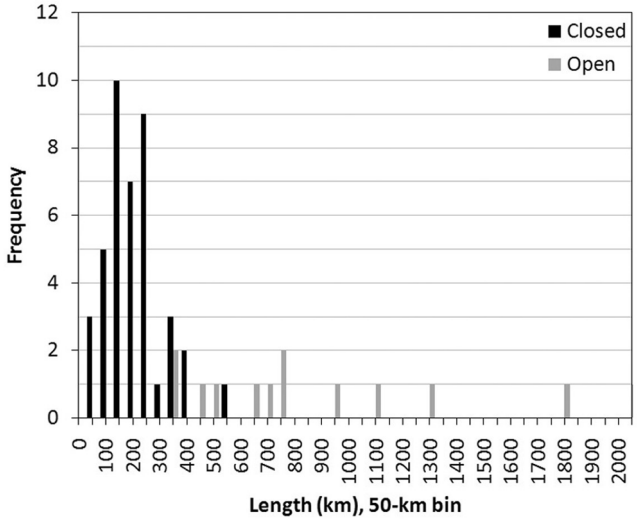

Figure 7. Histogram of the length of major valleys in closed and open watersheds (50 km bin). Watershed 13 has a length of 3350 km and is not shown.

this reason, differences are also apparent in the total relief of the open and closed watersheds (Figure 9). The anova rejected the hypothesis that that relief measurements from open and closed basins were drawn from the same probability distribution (p value = $1.31*10^{-8}$). We interpret Verde Vallis (W7) as formerly open, although a large fresh crater overlies its lower reach, so its terminal elevation is uncertain and may be too high at +700 m. Watersheds W28 and W36 drained to Hesperia Planum and likely did not continue across the low-relief, prevolcanic surface. Closed watersheds commonly trapped surface water at higher elevations, whereas the longer open watersheds drained to lower elevations.

[32] We find no statistically significant differences in gradient between the two groups at the 95% level (p value =

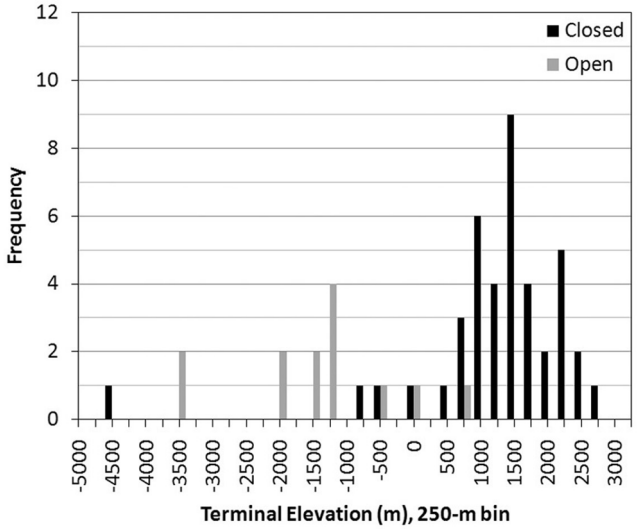

Figure 8. Histogram of the terminal elevations of closed and open watersheds (250 m bin), at the end of the incised stem valley.

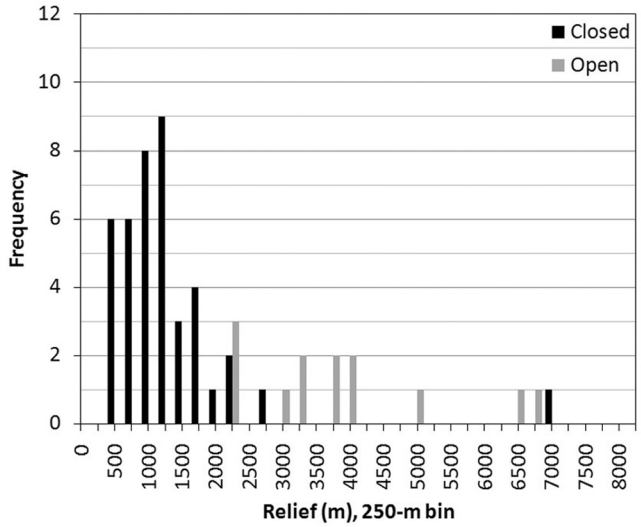

Figure 9. Histogram of the relief of closed and open watersheds (250 m bin), between the drainage divide and the end of the incised stem valley.

0.154). Measured dissected surfaces in these study areas had gradients of at least 0.002 (0.1°), whereas depositional surfaces have lower gradients than their respective contributing streams. The range in slope for these 54 watersheds fell between 0.002 and 0.017 (0.1–1°). Average slope measurements for each flow direction were: north, 0.0073 (15 watersheds); northeast, 0.0064 (6 watersheds); east, 0.0078 (9 watersheds); southeast, 0.0060 (1 watershed); south, 0.0064 (7 watersheds); southwest, 0.0064 (4 watersheds); west, 0.0060 (9 watersheds); and northwest, 0.0029 (3 watersheds). We did not measure drainage density for this project, but steeper surfaces above some critical length (or relief) appear to be more densely dissected.

[33] Given the variable topography of the Martian highlands, the longest stream in a given closed basin could be oriented in any direction. However, 11 of the 12 valleys > 400 km long in this study drained toward the west, northwest, north, or northeast (the 12th drained to Hellas). Of these 11 watersheds, 10 are located on slopes associated with the crustal dichotomy or Isidis. Ancient regional slopes associated with the crustal dichotomy appear to have been the most important factor in developing long valley networks on early Mars.

5. Discussion

5.1. Topographic Influences on Valley Networks

[34] Within our study areas we found that precursor topography influenced the occurrence and length of Martian valley networks, both where valleys are limited to isolated, preexisting slopes and where longer slopes generated enough runoff to overflow drainage divides and extend valleys farther down regional gradients. The statistically significant differences in length and relief between open and closed watersheds are due to incision of the longest valley networks on long regional slopes that predate the valleys, including the crustal dichotomy boundary, Isidis, and Hellas (Table 2). In contrast, the highland plateau is predominantly multibasinal with shorter valleys, and few of the enclosed basins overflowed during the Noachian-Hesperian time frame. The preservation of enclosed basins in the highlands may reflect their large floor areas relative to total watershed area, requiring higher ratios of precipitation to evaporation for overflow than occurred in most places. The extent of individual valley networks depends on the configuration of precursor slopes and does not appear to reflect substantial fluvial reworking of the landscape by the relict valleys, except perhaps on some localized, steep, densely dissected slopes. If valley development had significantly modified intercrater surfaces, then we would expect higher drainage densities (perhaps above unity) and better-graded longitudinal profiles than are consistently observed [e.g., *Carr*, 1995; *Grant*, 2000; *Cabrol and Grin*, 2001; *Aharonson et al.*, 2002; *Kereszturi*, 2005; *Stepinski and Stepinski*, 2005; *Luo and Howard*, 2005]. These observations are consistent with an arid paleoclimate (by terrestrial standards) during the Noachian Period, where precipitation was infrequent and/or low in magnitude.

[35] Martian valley networks dissect an older geomorphic surface, where a considerable amount of prior erosion had occurred, but where the long-wavelength (>100 km) topography is mostly Early to Pre-Noachian in age. Relict features of that older Noachian landscape, including the following, vary in age and effect. (1) The crustal dichotomy is the most extensive and topographically prominent element, and it predates all other relict geologic features on Mars [e.g., *Solomon et al.*, 2005; *Nimmo and Tanaka*, 2005]. The topography of the crustal dichotomy had the most influence along the cratered slope of the dichotomy boundary, which controlled the length and planform of valley networks [*Irwin and Watters*, 2010], including most of the longer (>400 km) open watersheds in this study. (2) In some areas, Early to Pre-Noachian, topographically prominent ridges or rises of unknown origin significantly influenced flow patterns. These features include elongated, possibly tectonic rises such as the ones noted above in Terra Sirenum, and broad areas of elevated topography like Terra Tyrrhena. (3) Large Noachian impact basins and related structures dominate the topography of the highland plateau. These basins include Hellas, Argyre, and Isidis, as well as many smaller (mostly early) Noachian, highly degraded basin structures [e.g., *Frey*, 2008]. Many of the latter impact basins also appear to have been mantled by ejecta from the Hellas, Argyre, and Isidis impacts, perhaps substantially modifying their topography. (4) Smaller Middle to Late Noachian impact craters provide local control on Noachian flow patterns, and some enclosed basins appear to result from later Noachian impacts damming a formerly integrated surface (e.g., W30) [*Irwin and Howard*, 2002]. Many enclosed watersheds on the highland plateau have divides related (at least in part) to Early or Pre-Noachian impact basins; structures related to Hellas, Argyre, or Isidis; and older topographic features of unknown origin. These divides limit watershed length, from divide to basin floor, to less than 300–400 km over most of the studied multibasin highland plateau. Fundamentally, long valley networks required long regional slopes that date to the Early Noachian Epoch or earlier, whereas impact basin topography kept valleys from extending more than 300–400 km on the plateau.

[36] The development of relatively few, large stem valleys (~10 km width and 500–1000 m depth) in the Martian highlands has never been adequately explained. Four large stem valleys in the Cimmeria west (Licus Vallis, W29), Cimmeria east (Durius (W45) and Al-Qahira Valles (W48)), and Sirenum (unnamed valley, W50) study areas all have a large contributing area, a watershed that concentrated runoff, a longitudinal convexity to incise (the crustal dichotomy boundary or a crater rim), and an uninterrupted slope toward the lowlands at some time prior to the Noachian-Hesperian transition. These factors likely contributed to the time and discharge available to incise these valleys, which did not require filling and overflowing large basins.

5.2. Noachian Landscape Evolution

[37] Throughout the Noachian Period the erosion of topographic highs, sediment transport down shallow gradients of 0.1–1°, and deposition in enclosed basins suggest that a gravity-driven process was primarily responsible for landscape denudation [e.g., *Craddock et al.*, 1997]. Impact craters on this surface were degraded in proportion to their relative age and size throughout the Noachian Period [*Craddock and Maxwell*, 1993]. However, streams did not incise deeply in most places, and the limited development of the relict Late Noachian valleys (e.g., poor longitudinal grading, low drainage density, short lengths) suggests that valley networks were not geologically long-lived features (see review by *Irwin et al.* [2008]). Conditions may not have favored entrenchment of rivers until the Late Noachian, or runoff may have been intermittent. The discussion below is speculative, but the scenario that we outline is consistent with the results of this study and other recent findings.

[38] The need to reconcile prolonged gravity-driven erosion of the highlands with limited entrenchment of valleys during most of the Noachian Period may yield useful insight into the paleoclimate. A critical observation is that the Martian highlands are undersaturated with both small craters and small valleys [e.g., *Neukum and Hiller*, 1981; *Grant*, 2000], so one cannot fully explain Noachian highland geomorphology using only cratering and fluvial erosion, either alone or jointly. Rivers entrench when their sediment transport capacity exceeds sediment supply. On Mars, the opposite condition may have prevailed through most of the Noachian Period, due to a typically arid paleoclimate without intense precipitation, where potential weathering outpaced fluvial erosion (a transport-limited condition). When precipitation and runoff did occur, there was no shortage of fines to transport in the relatively weak streams, which did not tend to incise deeply. This scenario is consistent with contributions from diffusional creep and aeolian transport in predominantly fluvial crater degradation [*Craddock et al.*, 1997]. A cratered landscape does not efficiently produce runoff, because of its relatively high infiltration capacity [*Grant and Schultz*, 1993] and radial centrifugal drainage pattern [*Pieri*, 1980], which disperses flow, increasing the need for preparatory weathering in crater degradation.

[39] The combination of weathering at some rate with relatively weak fluvial erosion would reduce promontories and create a relatively smooth, transport-limited surface with abundant mechanical and chemical weathering products, mixed with fresh basaltic materials exposed by post-Noachian impact gardening and aeolian abrasion. We do not necessarily imply that weathering rates were rapid by terrestrial standards, only that they outpaced fluvial erosion. A weathered highland surface is consistent with recent spectral data [e.g., *Mustard et al.*, 2008; *Murchie et al.*, 2009] and the poor preservation of small impact craters on highland intercrater plains relative to younger volcanic plains or indurated basin surfaces [e.g., *Malin and Edgett*, 2001]. There may not be a perfect terrestrial analog due to the thickness of the Earth's atmosphere and the potential for heavy rainfall, but an arid to hyperarid desert that experiences only intermittent, light rainfall and runoff (no intense storms by terrestrial standards) might be appropriate. Valley networks incised due to changing conditions around the Noachian-Hesperian transition, possibly an increase in either the magnitude or frequency of runoff, a decrease in weathering and the resulting sediment supply, formation of a duricrust that limited sediment supply and focused erosion, or some combination of these influences [*Howard et al.*, 2005].

5.3. Possible Topographic Controls on Precipitation

[40] Precursor topography was an important control on valley network development, but a regionally variable paleoclimate may have also had a significant influence. The single landmass of the Martian highlands covers ~55% of the surface, so a continentality effect would be expected, but the multibasin landscape on the plateau may have partly offset it. On Earth, most large enclosed basins have tectonic or glacial origins and are situated low in the landscape. In contrast, the Martian highland plateau includes a larger fraction of enclosed basins than do the surrounding regional slopes. Water precipitated at high elevations would have a longer residence time on the surface than it would at comparably high elevations on Earth, which are usually steep and drain efficiently toward the sea. Being unable to drain to distant basins, precipitation onto the Martian plateau would tend to pond and evaporate. Moreover, the high elevation near the South Pole would encourage ice accumulation during times of low obliquity, if Mars had an active water cycle. In this way, the Martian landscape could topographically and thermally retain water in the highlands, yielding a longer water cycle. Storage of water in the highlands would also reduce the evaporating surface area of northern basins, limiting former seas to lower and cooler elevations northward and making Mars more arid than it otherwise would have been for a given water inventory. We observe little evidence that early Mars, even at the peak of valley network activity around the Noachian-Hesperian transition, ever had a humid climate by terrestrial standards. Breaching of enclosed basins was rare and in most cases depended on large contributing areas [*Irwin et al.*, 2007; *Fassett and Head*, 2008b]. Regional differences in the precipitation/evaporation ratio may have also played a role in basin overflow, but this factor is unconstrained.

[41] The occurrence of long valley networks and overflowed basins on northward regional slopes suggests that, given a likely orographic effect of the crustal dichotomy on precipitation, much of the atmospheric humidity came from evaporation in the lowlands prior to Early Hesperian resurfacing [*Luo and Stepinski*, 2009]. If the humidity had come primarily from sources in the highlands or Tharsis and moved northward, then the northward slope should have been relatively arid due to descending air. However,

Noachian topographic features of less than ~10^6 m in extent and ~10^3 m in relief (to an order of magnitude) do not appear to have generated rain shadows, and the interior slopes of enclosed basins are often dissected, suggesting that precipitation resulted from atmospheric convection.

[42] *Hoke and Hynek* [2009] used crater retention ages within Naktong Vallis and other nearby watersheds to suggest that precipitation occurred in different watersheds (or even in different tributaries within the same network) over geologic time. Previously, *Irwin et al.* [2005] had noted that late stage integration of the Naktong/Scamander/Mamers network through previously enclosed basins resulted in incision of the eastern (main) branch of Naktong Vallis. The western branch may be older, as *Hoke and Hynek* [2009] suggested, but it requires only a change in the runoff production rate over time, rather than a local change in the location of precipitation, which would be more difficult to explain. Other geologic features here and elsewhere on Mars independently corroborate the former explanation [*Howard et al.*, 2005; *Irwin et al.*, 2005].

6. Summary

[43] Martian valley networks share many characteristics with terrestrial watersheds, but they are poorly developed by most quantitative measures, likely reflecting a short period of stream entrenchment into an older geomorphic surface around the Noachian-Hesperian transition (see review by *Irwin et al.* [2008]). Martian valleys also appear spatially clustered [*Gulick*, 2001], which may in part reflect topographic influences on Noachian hydrology. We investigated these possible controls in a study of watershed morphometry in nine study areas, which span a range of topographic and geographic locations in the Martian highlands (Figure 1b). These study areas include highland plateau surfaces and regional cratered slopes associated with impact basins and the crustal dichotomy boundary.

[44] Topographic features that formed throughout the Noachian Period were the primary control on the occurrence and length of Martian valley networks. These large-scale landforms include the crustal dichotomy, various broad rises of unknown origin, larger impact basins (most of which are strongly degraded and/or buried), and smaller degraded craters. These precursor slopes controlled the planform of valley networks, without being substantially regraded by the relict valleys in most locations. Most watershed lengths reflect the dimensions of a precursor slope, but some networks also collected enough water to overflow and breach some formerly enclosed basins, particularly on long regional slopes. Few enclosed basins on the highland plateau were breached during the Noachian Period. Comparing measurements of the longest open and closed watersheds within our nine study areas, we found statistically significant differences in length and relief, but not divide elevation or gradient between the two groups. Dissected surfaces had gradients of 0.1–1°. These results suggest that the length and relief of valley networks depended strongly on the presence of a preexisting slope, particularly the crustal dichotomy, Isidis, or Hellas, with longer slopes yielding longer valley networks.

[45] Late Noachian valley networks dissect an older geomorphic surface that formed throughout the Noachian Period along with impact crater degradation [e.g., *Grant*, 1987]. Streams did not commonly incise deep valleys prior to the Late Noachian Epoch, which suggests that the weathering rate and sediment supply exceeded the transport capacity (i.e., erosion was transport limited) for most of the Noachian Period. We propose a scenario wherein the Noachian paleoclimate was very arid, with weak and/or intermittent fluvial erosion and long intervals of weathering at some rate, until near the Noachian-Hesperian transition, when the valley networks developed. Aqueous weathering and fluvial erosion in this earlier climate would reduce topographic relief and transport sediment down low gradients into basins, as observed, but over long geologic time scales relative to terrestrial denudation. The current spectral signature of the highlands would be a mixture of weathered rocks and fresh basaltic surfaces exposed by post-Noachian impact gardening and aeolian abrasion, which is also consistent with orbiter and lander observations [e.g., *Bandfield et al.*, 2000; *Hartmann et al.*, 2001; *Christensen et al.*, 2001; *Arvidson et al.*, 2006; *Mustard et al.*, 2008; *Murchie et al.*, 2009].

[46] The ~6 km of relief across the crustal dichotomy boundary would have enhanced the relative humidity of air masses moving southward from the lowlands, with the opposite effect on highland air moving northward. It is thus likely that evaporation from the northern lowlands was an important source of water for long valley networks on the northward slope of the crustal dichotomy. The multibasin landscape on the highland plateau would have trapped surface water at higher, cooler elevations for much longer periods than is common on Earth, and the elevation of the South Pole would have created a thermal sink for atmospheric humidity. This retention of surface water in the highlands may have reduced the continentality effect observed on Earth. However, storage of water in the highlands would have also reduced the area of a putative northern lowland sea, which was presumably warmer than highland basins, thus limiting the water supply to slopes along the highland margin for any given global water inventory. The observation that large contributing watersheds were required to overflow most breached basins [*Irwin et al.*, 2007; *Fassett and Head*, 2008b] is consistent with the premise that early Mars was always fairly arid relative to the modern Earth, despite the important role of water in weathering and landscape denudation throughout the Noachian Period.

References

Aharonson, O., M. T. Zuber, D. H. Rothman, N. Schorghofer, and K. X. Whipple (2002), Drainage basins and channel incision on Mars, *Proc. Natl. Acad. Sci. U. S. A.*, *99*, 1780–1783, doi:10.1073/pnas.261704198.

Arvidson, R. E., et al. (2006), Overview of the Spirit Mars Exploration Rover Mission to Gusev Crater: Landing site to Backstay Rock in the Columbia Hills, *J. Geophys. Res.*, *111*, E02S01, doi:10.1029/2005JE002499.

Baker, V. R., and J. Partridge (1986), Small Martian valleys: Pristine and degraded morphology, *J. Geophys. Res.*, *91*(B3), 3561–3572, doi:10.1029/JB091iB03p03561.

Bandfield, J. L., V. E. Hamilton, and P. R. Christensen (2000), A global view of Martian surface compositions from MGS-TES, *Science*, *287*, 1626–1630, doi:10.1126/science.287.5458.1626.

Barnhart, C. J., A. D. Howard, and J. M. Moore (2009), Long-term precipitation and late-stage valley network formation: Landform simulations of Parana Basin, Mars, *J. Geophys. Res.*, *114*, E01003, doi:10.1029/2008JE003122.

Bhattacharya, J. P., T. H. D. Payenberg, S. D. Lang, and M. Bourke (2005), Dynamic river channels suggest a long-lived Noachian crater lake on Mars, *Geophys. Res. Lett.*, *32*, L10201, doi:10.1029/2005GL022747.

Cabrol, N. A., and E. A. Grin (2001), Composition of the drainage network on early Mars, *Geomorphology*, *37*, 269–287, doi:10.1016/S0169-555X(00)00087-8.

Carr, M. H. (1995), The Martian drainage system and the origin of valley networks and fretted channels, *J. Geophys. Res.*, *100*(E4), 7479–7507, doi:10.1029/95JE00260.

Carr, M. H. (2002), Elevations of water-worn features on Mars: Implications for circulation of groundwater, *J. Geophys. Res.*, *107*(E12), 5131, doi:10.1029/2002JE001845.

Carr, M. H., and F. C. Chuang (1997), Martian drainage densities, *J. Geophys. Res.*, *102*(E4), 9145–9152, doi:10.1029/97JE00113.

Carr, M. H., and G. D. Clow (1981), Martian channels and valleys: Their characteristics, distribution, and age, *Icarus*, *48*, 91–117, doi:10.1016/0019-1035(81)90156-1.

Christensen, P. R., et al. (2001), Mars Global Surveyor Thermal Emission Spectrometer experiment: Investigation description and surface science results, *J. Geophys. Res.*, *106*(E10), 23,823–23,871, doi:10.1029/2000JE001370.

Craddock, R. A., and A. D. Howard (2002), The case for rainfall on a warm, wet early Mars, *J. Geophys. Res.*, *107*(E11), 5111, doi:10.1029/2001JE001505.

Craddock, R. A., and T. A. Maxwell (1993), Geomorphic evolution of the Martian highlands through ancient fluvial processes, *J. Geophys. Res.*, *98*(E2), 3453–3468, doi:10.1029/92JE02508.

Craddock, R. A., T. A. Maxwell, and A. D. Howard (1997), Crater morphometry and modification in the Sinus Sabaeus and Margaritifer Sinus regions of Mars, *J. Geophys. Res.*, *102*(E6), 13,321–13,340, doi:10.1029/97JE01084.

Fassett, C. I., and J. W. Head III (2007), Layered mantling deposits in northeast Arabia Terra, Mars: Noachian-Hesperian sedimentation, erosion, and terrain inversion, *J. Geophys. Res.*, *112*, E08002, doi:10.1029/2006JE002875.

Fassett, C. I., and J. W. Head III (2008a), The timing of Martian valley network activity: Constraints from buffered crater counting, *Icarus*, *195*, 61–89, doi:10.1016/j.icarus.2007.12.009.

Fassett, C. I., and J. W. Head III (2008b), Valley network-fed, open-basin lakes on Mars: Distribution and implications for Noachian surface and subsurface hydrology, *Icarus*, *198*, 37–56, doi:10.1016/j.icarus.2008.06.016.

Forsberg-Taylor, N. K., A. D. Howard, and R. A. Craddock (2004), Crater degradation in the Martian highlands: Morphometric analysis of the Sinus Sabaeus region and simulation modeling suggest fluvial processes, *J. Geophys. Res.*, *109*, E05002, doi:10.1029/2004JE002242.

Frey, H. (2008), Ages of very large impact basins on Mars: Implications for the late heavy bombardment in the inner solar system, *Geophys. Res. Lett.*, *35*, L13203, doi:10.1029/2008GL033515.

Goldspiel, J. M., and S. W. Squyres (1991), Ancient aqueous sedimentation on Mars, *Icarus*, *89*, 392–410, doi:10.1016/0019-1035(91)90186-W.

Goldspiel, J. M., S. W. Squyres, and D. G. Jankowski (1993), Topography of small Martian valleys, *Icarus*, *105*, 479–500, doi:10.1006/icar.1993.1143.

Grant, J. A. (1987), The geomorphic evolution of eastern Margaritifer Sinus, Mars, in *Advances in Planetary Geology*, *NASA Tech. Memo., NASA TM-89871*, 1–268.

Grant, J. A. (2000), Valley formation in Margaritifer Sinus, Mars, by precipitation-recharged ground-water sapping, *Geology*, *28*, 223–226, doi:10.1130/0091-7613(2000)28<223:VFIMSM>2.0.CO;2.

Grant, J. A., and P. H. Schultz (1990), Gradational epochs on Mars: Evidence from west-northwest of Isidis Basin and Electris, *Icarus*, *84*, 166–195, doi:10.1016/0019-1035(90)90164-5.

Grant, J. A., and P. H. Schultz (1993), Degradation of selected terrestrial and Martian impact craters, *J. Geophys. Res.*, *98*(E6), 11,025–11,042, doi:10.1029/93JE00121.

Greeley, R., and J. E. Guest (1987), Geologic map of the eastern equatorial region of Mars, *U.S. Geol. Surv. Misc. Invest. Map*, *I-1802-B*, scale 1:15,000,000.

Gulick, V. C. (2001), Origin of the valley networks on Mars: A hydrological perspective, *Geomorphology*, *37*, 241–268, doi:10.1016/S0169-555X(00)00086-6.

Gulick, V. C., and V. R. Baker (1990), Origin and evolution of valleys on Martian volcanoes, *J. Geophys. Res.*, *95*(B9), 14,325–14,344, doi:10.1029/JB095iB09p14325.

Hartmann, W. K., J. Anguita, M. A. de la Casa, D. C. Berman, and E. V. Ryan (2001), Martian cratering 7: The role of impact gardening, *Icarus*, *149*, 37–53, doi:10.1006/icar.2000.6532.

Hauber, E., K. Gwinner, M. Kleinhans, D. Reiss, G. Di Achille, G.-G. Ori, F. Scholten, L. Marinangeli, R. Jaumann, and G. Neukum (2009), Sedimentary deposits in Xanthe Terra: Implications for the ancient climate on Mars, *Planet. Space Sci.*, *57*, 944–957, doi:10.1016/j.pss.2008.06.009.

Hoke, M. R. T., and B. M. Hynek (2009), Roaming zones of precipitation on ancient Mars as recorded in valley networks, *J. Geophys. Res.*, *114*, E08002, doi:10.1029/2008JE003247.

Howard, A. D. (1988), Introduction: Groundwater sapping on Mars and Earth, in *Sapping Features of the Colorado Plateau: A Comparative Planetary Geology Field Guide*, edited by A. D. Howard, R. C. Kochel, and H. R. Holt, *NASA Spec. Publ., NASA SP-491*, 1–5.

Howard, A. D. (2007), Simulating the development of Martian highland landscapes through the interaction of impact cratering, fluvial erosion, and variable hydrologic forcing, *Geomorphology*, *91*, 332–363, doi:10.1016/j.geomorph.2007.04.017.

Howard, A. D., J. M. Moore, and R. P. Irwin III (2005), An intense terminal epoch of widespread fluvial activity on early Mars: 1. Valley network incision and associated deposits, *J. Geophys. Res.*, *110*, E12S14, doi:10.1029/2005JE002459.

Irwin, R. P., III, and A. D. Howard (2002), Drainage basin evolution in Noachian Terra Cimmeria, Mars, *J. Geophys. Res.*, *107*(E7), 5056, doi:10.1029/2001JE001818.

Irwin, R. P., III, and T. R. Watters (2010), Geology of the Martian crustal dichotomy boundary: Age, modifications, and implications for modeling efforts, *J. Geophys. Res.*, *115*, E11006, doi:10.1029/2010JE003658.

Irwin, R. P., III, A. D. Howard, R. A. Craddock, and J. M. Moore (2005), An intense terminal epoch of widespread fluvial activity on early Mars: 2. Increased runoff and paleolake development, *J. Geophys. Res.*, *110*, E12S15, doi:10.1029/2005JE002460.

Irwin, R. P., T. A. Maxwell, and A. D. Howard (2007), Water budgets on early Mars: Empirical constraints from paleolake basin and watershed areas, Abstract 3400 presented at Seventh International Conference on Mars, Lunar and Planet. Inst., Pasadena, Calif.

Irwin, R. P., III, A. D. Howard, and R. A. Craddock (2008), Fluvial valley networks on Mars, in *River Confluences, Tributaries, and the Fluvial Network*, edited by S. Rice, A. Roy, and B. Rhoads, pp. 409–430, John Wiley, West Sussex, U. K.

Kereszturi, A. (2005), Cross-sectional and longitudinal profiles of valleys and channels in Xanthe Terra on Mars, *J. Geophys. Res.*, *110*, E12S17, doi:10.1029/2005JE002454.

Luo, W., and A. D. Howard (2005), Morphometric analysis of Martian valley network basins using a circularity function, *J. Geophys. Res.*, *110*, E12S13, doi:10.1029/2005JE002506.

Luo, W., and T. F. Stepinski (2009), Computer-generated global map of valley networks on Mars, *J. Geophys. Res.*, *114*, E11010, doi:10.1029/2009JE003357.

Malin, M. C., and K. S. Edgett (2001), Mars Global Surveyor Mars Orbiter Camera: Interplanetary cruise through primary mission, *J. Geophys. Res.*, *106*(E10), 23,429–23,570, doi:10.1029/2000JE001455.

Malin, M. C., and K. S. Edgett (2003), Evidence for persistent flow and aqueous sedimentation on early Mars, *Science*, *302*, 1931–1934, doi:10.1126/science.1090544.

Mangold, N., C. Quantin, V. Ansan, C. Delacourt, and P. Allemand (2004), Evidence for precipitation on Mars from dendritic valleys in the Valles Marineris area, *Science*, *305*, 78–81, doi:10.1126/science.1097549.

Masursky, H. (1973), An overview of geologic results from Mariner 9, *J. Geophys. Res.*, *78*(20), 4009–4030, doi:10.1029/JB078i020p04009.

Masursky, H., J. M. Boyce, A. L. Dial, G. G. Schaber, and M. E. Strobell (1977), Classification and time of formation of Martian channels based on Viking data, *J. Geophys. Res.*, *82*(28), 4016–4038, doi:10.1029/JS082i028p04016.

Moore, J. M. (1990), Nature of the mantling deposit in the heavily cratered terrain of northeastern Arabia, Mars, *J. Geophys. Res.*, *95*(B9), 14,279–14,289, doi:10.1029/JB095iB09p14279.

Moore, J. M., and A. D. Howard (2005), Large alluvial fans on Mars, *J. Geophys. Res.*, *110*, E04005, doi:10.1029/2004JE002352.

Moore, J. M., and D. E. Wilhelms (2001), Hellas as a possible site of ancient ice-covered lakes on Mars, *Icarus*, *154*, 258–276, doi:10.1006/icar.2001.6736.

Moore, J. M., A. D. Howard, W. E. Dietrich, and P. M. Schenk (2003), Martian layered fluvial deposits: Implications for Noachian climate scenarios, *Geophys. Res. Lett.*, *30*(24), 2292, doi:10.1029/2003GL019002.

Murchie, S. L., et al. (2009), A synthesis of Martian aqueous mineralogy after 1 Mars year of observations from the Mars Reconnaissance Orbiter, *J. Geophys. Res.*, *114*, E00D06, doi:10.1029/2009JE003342.

Mustard, J. F., et al. (2008), Hydrated silicate minerals on Mars observed by the Mars Reconnaissance Orbiter CRISM instrument, *Nature*, *454*, 305–309, doi:10.1038/nature07097.

Neukum, G., and K. Hiller (1981), Martian ages, *J. Geophys. Res.*, *86*(B4), 3097–3121, doi:10.1029/JB086iB04p03097.

Nimmo, F., and K. L. Tanaka (2005), Early crustal evolution of Mars, *Annu. Rev. Earth Planet. Sci.*, *33*, 133–161, doi:10.1146/annurev.earth.33.092203.122637.

Phillips, R. J., et al. (2001), Ancient geodynamics and global-scale hydrology on Mars, *Science*, *291*, 2587–2591, doi:10.1126/science.1058701.

Pieri, D. C. (1980), Geomorphology of Martian valleys, in *Advances in Planetary Geology*, edited by A. Woronow, *NASA Tech. Memo., NASA TM-81979*, 1–160.

Sharp, R. P., and M. C. Malin (1975), Channels on Mars, *Geol. Soc. Am. Bull.*, *86*, 593–609, doi:10.1130/0016-7606(1975)86<593:COM>2.0.CO;2.

Simon, A., and S. Darby (1999), The nature and significance of incised river channels, in *Incised River Channels: Processes, Forms, Engineering and Management*, edited by S. E. Darby and A. Simon, pp. 3–18, John Wiley, Chichester, U. K.

Solomon, S., and J. W. Head (1980), Lunar mascon basins: Lava filling, tectonics, and evolution of the lithosphere, *Rev. Geophys.*, *18*(1), 107–141, doi:10.1029/RG018i001p00107.

Solomon, S. C., et al. (2005), New perspectives on ancient Mars, *Science*, *307*, 1214–1220, doi:10.1126/science.1101812.

Stepinski, T. F., and A. P. Stepinski (2005), Morphology of drainage basins as an indicator of climate on early Mars, *J. Geophys. Res.*, *110*, E12S12, doi:10.1029/2005JE002448.

Wichman, R. W., and P. H. Schultz (1989), Sequence and mechanisms of deformation around the Hellas and Isidis impact basins on Mars, *J. Geophys. Res.*, *94*(B12), 17,333–17,357, doi:10.1029/JB094iB12p17333.

Wilson, S. A., A. D. Howard, J. M. Moore, and J. A. Grant (2007), Geomorphic and stratigraphic analysis of Crater Terby and layered deposits north of Hellas basin, Mars, *J. Geophys. Res.*, *112*, E08009, doi:10.1029/2006JE002830.

Wilson, S. A., J. M. Moore, A. D. Howard, and D. E. Wilhelms (2010), Evidence for ancient lakes in the Hellas region, in *Lakes on Mars*, edited by N. Cabrol and E. Grin, pp. 195–222, Elsevier, Oxford, U. K.

R. A. Craddock, Center for Earth and Planetary Studies, National Air and Space Museum, Smithsonian Institution, MRC 315, 6th St. at Independence Ave. SW, Washington, DC 20013, USA.

H. L. Flemming, MDA Information Systems Inc., 820 W. Diamond Ave., Ste. 300, Gaithersburg, MD 20878, USA.

A. D. Howard, Department of Environmental Sciences, University of Virginia, P.O. Box 400123, Charlottesville, VA 22904, USA.

R. P. Irwin III, Planetary Geodynamics Laboratory, NASA Goddard Space Flight Center, Code 698, Greenbelt, MD 20771, USA. (irwin@psi.edu)